Fish and Shellfish Immunology 90 (2019) 275–287

Contents lists available at ScienceDirect

Fish and Shellfish Immunology

journal homepage: www.elsevier.com/locate/fsi

Full length article

A janus kinase from *Scylla paramamosain* activates JAK/STAT signaling pathway to restrain mud crab reovirus

Hengwei Deng[a,b], Xiaopeng Xu[a,b], Lei Hu[a,b,1], Jingjing Li[a,b], Dandan Zhou[a,b], Shanshan Liu[a,b], Panpan Luo[a,b], Jianguo He[a,b,**], Shaoping Weng[a,b,*]

[a] State Key Laboratory for Biocontrol / School of Life Sciences, Sun Yat-sen University, Guangzhou, PR China
[b] Guangdong Provice Key Laboratory for Aquatic Economic Animals, Sun Yat-sen University, PR China

ARTICLE INFO

Keywords:
Janus kinase
JAK/STAT pathway
Scylla paramamosain
MCRV
Antiviral immune

ABSTRACT

JAK/STAT signaling pathways are associated with the innate immune system and play important roles in mediating immune responses to virus infection. In this study, a Janus kinase gene from *Scylla paramamosain* (*Sp*JAK) was cloned and characterized. The full length of *Sp*JAK mRNA contains a 5′ untranslated region (UTR) of 304 bp, an open reading frame of 3300 bp and a 3′ UTR of 302 bp. The *Sp*JAK protein contains seven characteristic JAK homology domains (JH1 to JH7) and showed 60% identity (78% similarity), 20% identity (35% similarity), and 21% identity (37% similarity) to the *Litopenaeus vannamei* JAK (*Lv*JAK) protein, the *Drosophila melanogaster* hopscotch protein, and the *Homo sapiens* JAK2 protein, respectively. The mRNA of *Sp*JAK showed high expression in the brain and nerve but low expression in the hemocyte and muscle. Moreover, the expression of *Sp*JAK was significantly upregulated by stimulation with mud crab reovirus (MCRV), poly(I:C), and *Vibrio parahaemolyticus*. *Sp*JAK significantly activated the STAT of *S. paramamosain* (*Sp*STAT) to translocate to the nucleus of *Drosophila* Schneider 2 cells. *Sp*JAK significantly enhanced the activity of the promoter of the WSSV wsv069 gene that was activated significantly by *Sp*STAT by acting on the STAT-binding DNA motif. These results suggest that *Sp*JAK activates the JAK/STAT pathway. Furthermore, silencing *Sp*JAK *in vivo* resulted in the high mortality rate of MCRV-infected mud crabs and increased the viral load in tissues. Hence, *Sp*JAK could play an important role in defense against MCRV in mud crab.

1. Introduction

The mud crab, *Scylla paramamosain*, is an economically important marine species cultured in Southern China [1], and the total aquaculture production of this species reached 149000 tons in 2016 [2]. With the development of intensive culture, various diseases have severely affected the production of mud crab. The “sleeping disease” caused by mud crab reovirus (MCRV) resulted in 70% mortality of cultured mud crab at the affected farms and has resulted in large economic losses in China since 2004 [1,3].

Innate immunity is a central defense against invading pathogens in invertebrates, such as crustaceans and insects, which generally lack acquired immunity and highly rely on innate immunity [4]. The Janus kinase (JAK)/signal transducers and activators of transcription (STAT) pathway was first identified as a cytokine-induced signaling pathway in mammals and has been widely characterized from humans to *Drosophila* [5,6]. The JAK/STAT signaling pathway is involved in multiple biological processes, including hemopoietic development and differentiation, embryonic development, tissue homoeostasis, and innate and adaptive immunity [5,7]. JAK/STAT signaling mediates several innate immunity processes, including activation of neutrophils and macrophages, regulation of inflammatory responses, and wound repair [5,7]. In general, JAK/STAT signaling is a canonical mammalian antiviral signaling pathway that is an important component of the interferon response [8].

In the canonical mode of JAK-STAT signaling, the activation of the pathway is initiated by binding of a peptide ligand to transmembrane receptors [9]. This phenomenon leads to receptor dimerization and cross-activation of receptor-associated JAK kinases, which in turn phosphorylate tyrosine residues in the cytoplasmic tail of the receptor [9]. These phosphotyrosine residues function as docking sites for latent cytoplasmic STAT proteins, which are then phosphorylated by JAK. The

* Corresponding author. School of Life Sciences, School of Marine Sciences, Sun Yat-sen University, Guangzhou, 510275, PR China.
** Corresponding author. State Key Laboratory for Biocontrol / School of Life Sciences, Sun Yat-sen University, Guangzhou, PR China.
E-mail addresses: lsshjg@mail.sysu.edu.cn (J. He), lsswsp@mail.sysu.edu.cn (S. Weng).
[1] Lei Hu is a master of College of Animal Science, South China Agriculture University, Guangzhou, PR China.

https://doi.org/10.1016/j.fsi.2019.03.056
Received 28 September 2018; Received in revised form 24 March 2019; Accepted 25 March 2019
Available online 29 March 2019

Table 1
Summary of primers in this study.

Name	Sequence (5′–3′)
spliced and verified	
*Sp*JAK-F	TTGCGGTTCAAGCCATACACTC
*Sp*JAK-R	ACACACAGCCATCACAGGTC
RACE	
*Sp*JAK-3′RACE-A	GGACATTGCTGAGGGGATGGATTAC
*Sp*JAK-3′RACE-B	AACCCAACAAGGGGAACTACTACATCAG
*Sp*JAK-3′RACE-C	TGCCTTGCCTCTGCCTTGGTATG
*Sp*JAK-5′RACE-A	GCACACCAGTCTTGCGGGACACCT
*Sp*JAK-5′RACE-B	GGGTGTTCGGTGTGGTAGGGGTCAA
*Sp*JAK-5′RACE-C	CACCACCAGACCCAGACCATCCTCAG
Real-time RT-PCR	
*Sp*JAK-Q-F	CCACCTTCAAGACTCCAGGGATTTCTACAG
*Sp*JAK-Q-R	CCTGCTGGACGAGGCACAGATGAG
*Sp*STAT-Q-F	CACCAGATCAAGGAGTGTGAGCGACA
*Sp*STAT-Q-R	GGTGACAAGTGAGGACAGCAAGCGA
18SrRNA-F	AGTCGTAACAAGGTTTCCGTAGGTG
18SrRNA-R	GCGACCACCCACTATTTGTATTAGC
Absolute real-time quantitative PCR	
S12-Q-F	ATCGGAGGACAACTCACTACCACG
S12-Q-R	CATCTCCCTCGCCATATCCAATCT
Protein expression	
*Sp*JAK-F	GTACCTACTAGTCCAGTGTGGTGGATCAAAATGCTGACCGTCGCCTTCAATGGAG
*Sp*JAK-R	TTCGAAGGGCCCTCTAGACTCGAGCAGGTCCTCCTCCTGAAGTTCCTTCACTTG
*Sp*JAKmut1-F	GTACCTACTAGTCCAGTGTGGTGGATCAAAATGAATGTGCTGCGTGATGAAG
*Sp*JAKmut1-R	TTCGAAGGGCCCTCTAGACTCGAGCAGGTCCTCCTCCTGAAGTTCCT
*Sp*JAKmut2-AF	GTACCTACTAGTCCAGTGTGGTGGATCAAAATGCTGACCGTCGCCTTCAA
*Sp*JAKmut2-AR	ACAAAGTCACGAATCATTCCCCCCCGGCAGAGATCAAAGGTCC
*Sp*JAKmut2-BF	GGACCTTTGATCTCTGCCGGGGGGGAATGATTCGTGACTTTGT
*Sp*JAKmut2-BR	TTCGAAGGGCCCTCTAGACTCGAGCAGGTCCTCCTCCTGAAGTTCCTT
*Sp*JAKmut3-AF	GTACCTACTAGTCCAGTGTGGTGGATCAAAATGCTGACCGTCGCCTTCAA
*Sp*JAKmut3-AR	CGCCATTCTGCTGCTGTAAGTCGGATGTGAGGTGCGACATACTGAT
*Sp*JAKmut3-BF	ATCAGTATGTCGCACCTCACATCCGACTTACAGCAGCAGAATGGCG
*Sp*JAKmut3-BR	TTCGAAGGGCCCTCTAGACTCGAGCAGGTCCTCCTCCTGAAGTTCCTT
*Sp*STAT-F	CGGAATTCATCAAAATGTCCCTTTGGAATAGAGCACAA
*Sp*STAT-R	CCGCTCGAGCTGTTGCTTCATAAAGTTGGTATGG
Primers used for EMSA probes	
WSV069-F	ATGTGGCTAATGGAGAATTGTC
WSV069-R	CTTGAGTGGAGAGAGAGAGCTAGT
dsRNA templates amplification	
DsRNA-*Sp*JAK-T7F	GGATCCTAATACGACTCACTATAGGACTGGAGTTTCGTTTGCGGT
dsRNA-*Sp*JAK-R	GTGTTCGGTGTGGTAGGGGT
dsRNA-*Sp*JAK-F	ACTGGAGTTTCGTTTGCGGT
dsRNA-*Sp*JAK-T7R	GGATCCTAATACGACTCACTATAGGGTGTTCGGTGTGGTAGGGGT
dsRNA-eGFP-T7F	GGATCCTAATACGACTCACTATAGGACGGCAAGCTGACCCTGAAG
dsRNA-eGFP-R	GACTGGGTGCTCAGGTAGTGG
dsRNA-eGFP-F	ACGGCAAGCTGACCCTGAAG
dsRNA-eGFP-T7R	GGATCCTAATACGACTCACTATAGGGACTGGGTGCTCAGGTAGTGG

phosphorylated STAT proteins dimerize via Src-homology 2 (SH2)-domain phospho-tyrosine interactions and translocate to the nucleus, where they function as transcriptional activators to induce the expression of target genes [9–12]. Genes regulated by the mammalian JAK-STAT pathway also include positive and negative regulators, which modulate the magnitude and/or duration of signaling [10,12,13]. The activated STAT proteins drive their own expression to form a positive feedback loop or compensate for activation-induced STAT degradation. Several negative regulators of the pathway have been identified and are believed to be responsible for "turning off" JAK-STAT signaling after activation [10,12,13]. In insects, the *Drosophila* JAK-STAT pathway contains a single JAK (Hopscotch or Hop) and a single STAT (STAT92E) protein, which are highly homologous to *Homo sapiens* JAK2 and STAT5, respectively [14,15]. The core components of the fly JAK-STAT pathway function in a single linear manner that is typical of canonical JAK-STAT signaling. Moreover, the *Drosophila* JAK-STAT pathway is autoregulated by inducing positive and negative regulators [13]. As a positive regulator, STAT92E, similar to mammalian STATs [12], is transcriptionally induced by JAK-STAT signaling [16]. As negative regulators, SOCS36E (a SOCS protein) [17–19] and protein phosphatase PTP61F [20] are transcriptionally induced by STAT, which then inhibit JAK and STAT92E by either hindering phosphorylation or dephosphorylation [17–20].

In vertebrates, viral infections sensed by PRRs (such as TLRs) trigger inflammation and type I interferon (IFN) responses [21,22]. The JAK-STAT signaling pathways are activated by type I IFNs via a type I IFN receptor and lead to the production of interferon-stimulated genes (ISGs) [21,22]. ISGs, such as IRFs, 2′5′-oligoadenylate synthase, dsRNA-dependent protein kinase PKR, and adenosine deaminase, RNA-specific (ADAR), mediate the inhibition of viral replication, the clearance of virus-infected cells, and the induction of nonspecific antiviral responses [21,22]. The JAK/STAT signaling pathway induces antiviral activity in insects, including *Drosophila* and mosquitoes [23–25]. Mutants for JAK are susceptible to *Drosophila* C virus (DCV) and cricket paralysis virus (CrPV) and exhibit either no or a weak phenotype for other viruses, including solenopsis invicta virus(SINV), vesicular stomatitis virus (VSV), *Drosophila* X virus(DXV), and invertebrate iridescent virus 6(IIV-6) [23,25]. This finding suggests that the JAK/STAT pathway-dependent inducible response is virus specific. In *Drosophila* and mosquitoes, knockdown and mutation of JAK promote viral infection, suggesting that the JAK-STAT pathway elicits antiviral response. The JAK-STAT signaling pathways are also considered as part of the antiviral response

mechanisms in other insects [25]. In Crustacea, a similar JAK-STAT signaling pathway was characterized in shrimp [26–28]. The expression level of the members of the JAK-STAT signaling pathway, such as JAK, SOCS, and STAT, was induced by WSSV or poly(I:C) [28–30]. After WSSV infection, the activated STAT translocated from the cytoplasm to the nucleus in the primary culture cells of shrimp. Shrimp STAT was found to be activated in response to WSSV infection [26]. In *Litopenaeus vannamei*, *Lv*JAK could be regulated by JAK itself or (and) STAT, indicating that *Lv*JAK is the JAK/STAT pathway target gene and could function as a positive regulator to form a positive feedback loop. In addition, the silencing of *Lv*JAK caused high rates of mortality and WSSV genome replication, indicating that *Lv*JAK could play an important role in defense against WSSV [29].

Innate humoral immune response is mainly mediated by three immune signaling pathways, namely, Toll pathway, IMD pathway, and JAK/STAT pathway [9,10]. In crab, the Toll pathway regulates the expression of anti-lipopolysaccharide factor genes to counter invading microbes [31]. Five homologs of Toll pathway components have been identified in mud crab; these components are Toll [32], MyD88 [33], Tube, Pelle [34], and TRAF6 [31]. Peroxinectin [35] and Epigallocatechin-3-gallate [36] could inhibit WSSV replication in mud crab. However, limited information is known about the roles of the JAK/STAT pathway during the immune response of mud crab against viral infection. In this study, a JAK gene was identified and cloned from *S. paramamosain*. The mRNA expression and potential functions of the gene were examined during MCRV infection.

2. Materials and methods

2.1. Cloning of SpJAK cDNA

Total RNA was extracted from mud crab gills by using RNeasy Mini Kit (QIAGEN, Germany) and reverse transcribed into cDNA by using a PrimeScript™ RT reagent kit with a gDNA Eraser (Perfect Real Time, TaKaRa, Japan). Based on our previously reported high-throughput *S. paramamosain* transcriptome data [37], some EST sequences annotated as putative Janus kinase were retrieved and used to design specific primers (Table 1) for cloning the successional sequence of the *Sp*JAK gene. The cDNA library for rapid amplification of cDNA ends (RACE) was constructed using the SMARTer™ RACE cDNA Amplification kit (Clontech, Japan) according to methods reported in a previous research [38]. The first round of RACE PCR amplification was performed with Universal Primer A Mix and *Sp*JAK specific primers, namely, 5′RACE-A, 5′RACE-B, 3′RACE-A, and 3′RACE-B (Table 1), by using the touch-down PCR program. The second round of RACE PCR amplification was performed with Nested Universal Primer A and *Sp*JAK 5′RACE-C and 3′RACE-C primer by using the corresponding first round PCR product (200-fold dilution) as template with the standard PCR program. The same band of the second PCR products was cloned into the pMD-19T vector (TaKaRa, Japan). Eight positive clones were selected for sequencing.

2.2. Sequence and phylogenetic tree analysis

The protein sequences of JAK homologs from other species in the Genbank database were retrieved using the BLAST program (http://www.ncbi.nlm.nih.gov/BLAST/). The protein structural domains of *Sp*JAK were analyzed using InterPro Scan (http://www.ebi.ac.uk/InterProScan/) and SMART program (http://smart.embl-heidelberg.de/). Sequence alignments were performed using Clustal X v2.0 program [39] and visualized using GeneDoc software. Identities and similarities between *Sp*JAK and JAK homologs were added. Phylogenetic trees were constructed based on the deduced amino acid sequences of *Sp*JAK and other known JAK proteins by using MEGA 5.0 software [40] with neighbor-joining method. Amino acid substitution type and Poisson model and bootstrapping procedure with a minimum of 1000 bootstraps were applied.

2.3. Plasmid constructions

The open reading frame (ORF) of *Sp*JAK was mutated using overlapping PCR to generate JAKmut1 with the FERM domain (19–199) deletion mutation, JAKmut2 with the Src homology 2 domain (SH2, 303–389) deletion mutation, and JAKmut3 with the first tyrosine kinase catalytic domain (TyrKc, 450–718) deletion mutation. The full lengths of JAK, JAKmut1, JAKmut2, and JAKmut3 were cloned into pAc5.1/V5-His A by using Hieff Clone™ Multi One Step Cloning Kit (Yeasen, China) to express V5-tagged protein. The full lengths of STAT (GenBank Accession MH924352) were cloned into the *Eco*R I/*Xho* I sites of pAc5.1/V5-His A or pAc5.1-GFP vectors, which were reconstructed by cloning the GFP coding sequence into the *Drosophila* expression vector pAc5.1/V5-His A (Invitrogen) at *Bst*BI/*Pme*I sites to replace the V5-His tag. These expression vectors were inserted with a *Drosophila* Kozak consensus sequence (ATCAAA) before the ATG initiation codon for efficient initiation of translation [41]. The primer sequences are listed in Table 1. The PGL3-wsv069 reporter gene plasmid containing the full length of the wsv069 promoter was obtained from our laboratory [42].

2.4. Subcellular localization

Drosophila Schneider 2 (S2) cells were cultured at 28 °C in *Drosophila* serum-free Medium (Invitrogen) supplemented with 10% fetal bovine serum (Invitrogen). S2 cells were transfected with the V5-tagged plasmid of *Sp*JAK and its mutants by using FuGENE Transfection Reagent (Promega). After 48 h, S2 cells were transfected with the plasmids of *Sp*JAK and its mutants. Indirect immunofluorescence was used to analyze the subcellular localization of *Sp*JAK. Immunostaining was performed using an *anti*-V5 antibody (1:500). The cells were then incubated with Alexa Fluor 488-labeled goat anti-mouse antibody (1:500), stained with Hochest 33342 (Beyotime, China; 1:1000), and visualized with a confocal laser scanning microscope (Leica TCS-SP5, Germany).

S2 cells were co-transfected with equal-quality *Sp*STAT-GFP and V5-tagged plasmid of *Sp*JAK or its mutant and pAc5.1/V5-His A as control. After 48 h, indirect immunofluorescence was used to analyze the subcellular localization of *Sp*JAK or its mutant and *Sp*STAT. Immunostaining was performed using an *anti*-V5 antibody (1:500). The cells were then incubated with Alexa Fluor 555-labeled goat anti-rabbit antibody (1:500), then stained with Hochest 33342 (Beyotime, China; 1:1000) and visualized on a confocal laser scanning microscope (Leica TCS-SP5, Germany). Meanwhile, the other part of the cells were harvested for western blotting to detect whether or not *Sp*JAK was expressed in the cells. Total cell lysates were harvested and separated on 10% sodium dodecylsulfate (SDS)-polyacrylamide gels and transferred to polyvinylidene difluoride (PVDF) membranes. The membrane was blocked with 5% skim milk in phosphate buffered saline (PBS) for 1 h and then incubated at room temperature with an *anti*-V5 tag monoclonal antibody (1: 5000; Abcam). The signals were detected using Immobilon Western Chemiluminescent HRP Substrate (Millipore, MA, USA).

2.5. Dual-luciferase reporter assays

For DNA transfection, S2 cells were seeded into a 24-well plate (TPP, Switzerland) and transfected using the FuGENE Transfection Reagent (Promega) according to the manufacturer's recommendation until the cells grew to 50%–80% confluency. For dual-luciferase reporter assays, S2 cells in each well were co-transfected with 0.3 μg of the reporter gene plasmids, 0.02 μg of the pRL-TK *Renilla* luciferase plasmid (Promega), and 0.3 μg of the expression plasmids or empty pAc5.1/V5-His A plasmid (as a control). The pRL-TK *Renilla* luciferase

plasmid was used as internal control. At 48 h post transfection, dual-luciferase reporter assays were performed to calculate the relative ratio of firefly and *Renilla* luciferase activities according to the manufacturer's instructions.

2.6. Electrophoretic mobility shift assay (EMSA)

The specific primers of wsv069 promoter were designed and listed in Table 1. The full length of the wsv069 promoter was amplificated and purified. The double-stranded DNA of wsv069 promoter was labeled with biotin according to the protocols described in Pierce Biotin 3′ End DNA Labeling Kit (Thermo Scientific). Cell lysates were prepared from S2 cells transfected with pAC5.1-V5-*Sp*JAK plasmid using cell lysis buffer (50 mM Tris, pH 7.8; 150 mM NaCl and 1% Nonidet P-40) by addition with protease inhibitors (Calbiochem). In the EMSA, biotin-labeled DNA probes were incubated with cell extracts containing *Sp*JAK and Trx protein (as control) at room temperature in the presence of binding buffer from EMSA/gel-shift kit (Thermo Scientific). For competition experiment, cell extracts and Trx protein were preincubated with the wild probes (unlabeled) for 30 min before addition of the biotin-labeled probes. After the binding reactions, DNA-protein complexes were resolved by electrophoresis in 6% native acrylamide gel and transferred to a nylon membrane (GE Healthcare). The membrane was immediately cross-linked with UV-light and detected with Light-Shift Chemiluminescent EMSA Kit from Thermo Scientific.

2.7. Real-time RT-PCR analysis of SpJAK expression

Healthy mud crabs (*S. paramamosain*) weighing 80–100 g each were obtained from a farm (Nansha, Guangdong Province, China) and maintained in aquarium facilities as described previously [1]. Hemocyte, gill, heart, hepatopancreas, intestine, muscle, ganglion, stomach, eyestalk, and brain were sampled. Each tissue was pooled from three crabs and stored in RNAlater (Ambion, USA). RNA was extracted and reverse transcribed into cDNA as described above. The expression levels of *Sp*JAK were detected by real-time RT-PCR on a LightCycler480 system (Roche) with primers *Sp*JAK-Q-F/R (Table 1) and calculated using Livak ($2^{-\triangle\triangle CT}$) method after normalization to *S. paramamosain* 18S Ribosomal RNA (18S rRNA, Accession No. KC902763.1).

For the challenge experiments, mud crabs were divided into six experimental groups and injected with the following in their swimming leg: MCRV at 10^4 copies/g body weight, lipopolysaccharide (LPS, purified from *Escherichia coli* 0111:B4, Sigma) at 0.4 μg/g body weight, 0.4 μg/g polyinosinic:polycytidylic acid (Poly I:C, Sigma), 2×10^4 CFU/g *Staphylococcus aureus*, and 2×10^4 CFU/g CFU *Vibrio parahaemolyticus*. In the control group, each mud crab was injected with 50 μL of PBS. Three mud crabs were randomly selected from each group, and their gills were sampled at 0, 4, 8, 12, 24, 36, 48, 72, and 96 h post injection (hpi). Total RNA was extracted from mud crab gills and reverse transcribed to cDNA. *Sp*JAK mRNA was detected by real-time RT-PCR.

2.8. Knockdown of SpJAK expression

The double-stranded RNAs (dsRNAs) of *Sp*JAK and GFP (as a control) were produced through *in vitro* transcription using RiboMAX™ Large Scale RNA production System-T7 (Promega, USA) with specific primers (Table 1). The lengths of *Sp*JAK and GFP dsRNA are 463 and 499 bp, respectively. The final concentration of dsRNA was diluted with RNase-free water to 400 mg/mL. The experimental groups were injected with 200–250 μL of *Sp*JAK dsRNA (1 μg/g crab), and the control group was injected with GFP dsRNA and PBS to investigate RNA interference efficiency. At 48 h post injection, total RNA was extracted from the gills and reverse transcribed into cDNA as the template for RT-PCR to measure RNA interference efficiency. The relative mRNA levels of *Sp*JAK and *Sp*STAT were determined with 18S rRNA as internal control.

2.9. MCRV and PBS challenge experiments in SpJAK-knockdown mud crab

A total of 160 healthy *S. paramamosain* (average 100 g) were divided into three groups, with 40 crabs injected with dsRNA-*Sp*JAK, 40 crabs injected with dsRNA-GFP, and 80 crabs injected with PBS as control. At 48 h later, the surviving mud crabs in the PBS-injected group were mock-challenged with PBS as control and others groups were injected with MCRV (2×10^4 copies/g). The mud crabs were kept in culture flasks for about 5 days following infection. Cumulative mortality was recorded every 8 h. Differences in mortality levels among treatments were tested for statistical significance through Kaplan–Meier plot (log-rank χ^2 test) using GraphPad Prism software.

For the MCRV challenge test, a parallel experiment was performed to monitor MCRV replication. In brief, gill tissues (0.03 g) were sampled from nine surviving mud crabs at 48, 72, and 96 h post infection and subjected to total RNA extraction. MCRV copies were measured by absolute real-time quantitative PCR (qPCR) using primers S12-Q-F/R (Table 1) for the MCRV S12 gene as previously reported [3]. A standard curve was generated from serial dilutions (10^{10}, 10^9, 10^8, 10^7, 10^6, 10^5, 10^4, and 10^3 copies) of plasmids containing the S12 fragment. The reaction system and PCR were performed following the steps of real-time RT-PCR. Absolute qPCR was carried out using four replicates per sample. The MCRV copy numbers in 1 g of mud crab gills were calculated.

3. Results

3.1. Cloning and characterization of SpJAK

Three EST sequence fragments (550, 1499, and 877 bp) annotated as a putative Janus kinase were retrieved from high-throughput *S. paramamosain* transcriptome data [37]. The 3092 bp successional sequence of the *Sp*JAK gene were obtained using specific primers (Table 1). Other regions of *Sp*JAK were obtained by 5′- and 3′-RACE. The *Sp*JAK transcript is 3906 bp long and consists of a 304 bp 5′-untranslated region (UTR), a 302 bp 3′-untranslated region, and a 3300 bp ORF encoding a 1099 amino acid protein with a calculated molecular weight of 125.4 kDa (GenBank Accession MH598509, Fig. 1A). Conserved domain analysis showed that *Sp*JAK contains a FERM domain of 194 amino acids in the N-terminal region, an Src homology 2 domain (SH2) of 89 amino acids located at 314–402, and two tyrosine kinase catalytic domains (TyrKc) located at 448–698 and 836–1091 in the C-terminal region (Fig. 1). *Sp*JAK contains the conserved primary structure, namely, JAK homology regions (JHs), from JH1 to JH7, numbered from the carboxyl to the amino terminus (Figs. 1B and 2). The amino acid sequences of *Sp*JAK were aligned with the *D. melanogaster* protein and *H. sapiens* JAK family members (Fig. 2). *Sp*JAK showed 60% identity (78% similarity) to the *L. vannamei* JAK (*Lv*JAK), 20% identity (35% similarity) to the *D. melanogaster* HOP protein (*Dm*JAK), and 21% identity (37% similarity) to the *H. sapiens* JAK2 protein (HsJAK2, Fig. 2).

3.2. Phylogenetic analysis of the SpJAK protein

To determine the evolutionary position of the JAK proteins of *S. paramamosain*, we constructed phylogenetic trees using NJ method. The full length sequences of the JAK family proteins from humans, *Drosophila*, and other species were phylogenetically analyzed. The constructed phylogenetic tree indicates that all the JAK proteins used in this study were separated into the Insecta, Crustacea, Urochorda, and Vertebrata groups. *Sp*JAK was nearly clustered with crustacean proteins, namely, *L. vannamei* JAK, *Artemia franciscana* JAK (*Af*JAK), and *Daphnia pulex* JAK (*Dp*JAK) (Fig. 3).

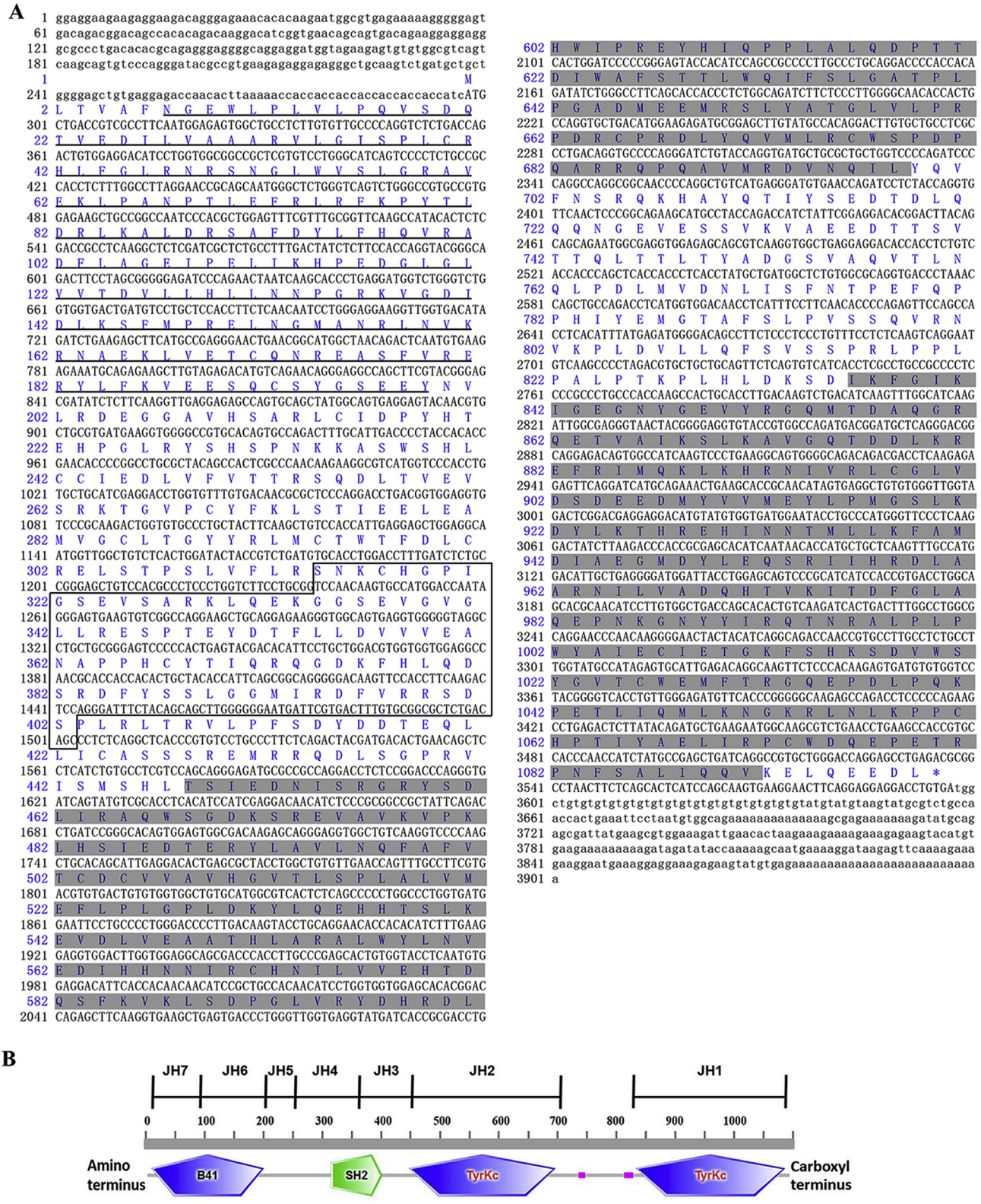

Fig. 1. Sequence analysis of *Sp*JAK gene. (A)Nucleotides and amino acids were numbered on the left of the sequences. The ORF of the nucleotide sequence was shown in upper-case letters, while the 5′ and 3′UTR sequences were shown in lowercase. Amino acid sequence was represented with one-letter codes above the nucleotide sequence. The FERM domain in the N-terminal was underlined, the Src homology 2 domain (SH2) was boxed with black line, and two tyrosine kinase catalytic domains (TyrKc) were shaded. (B) Domain structure of *Sp*JAK. *Sp*JAK proteins have four distinct domains, consisting of FERM (B41), SH2-like, and two tyrosine kinase catalytic domains (TyrKc). An alternative nomenclature for the putative domains is as seven defined regions of homology called Janus homology (JH) domains 1–7.

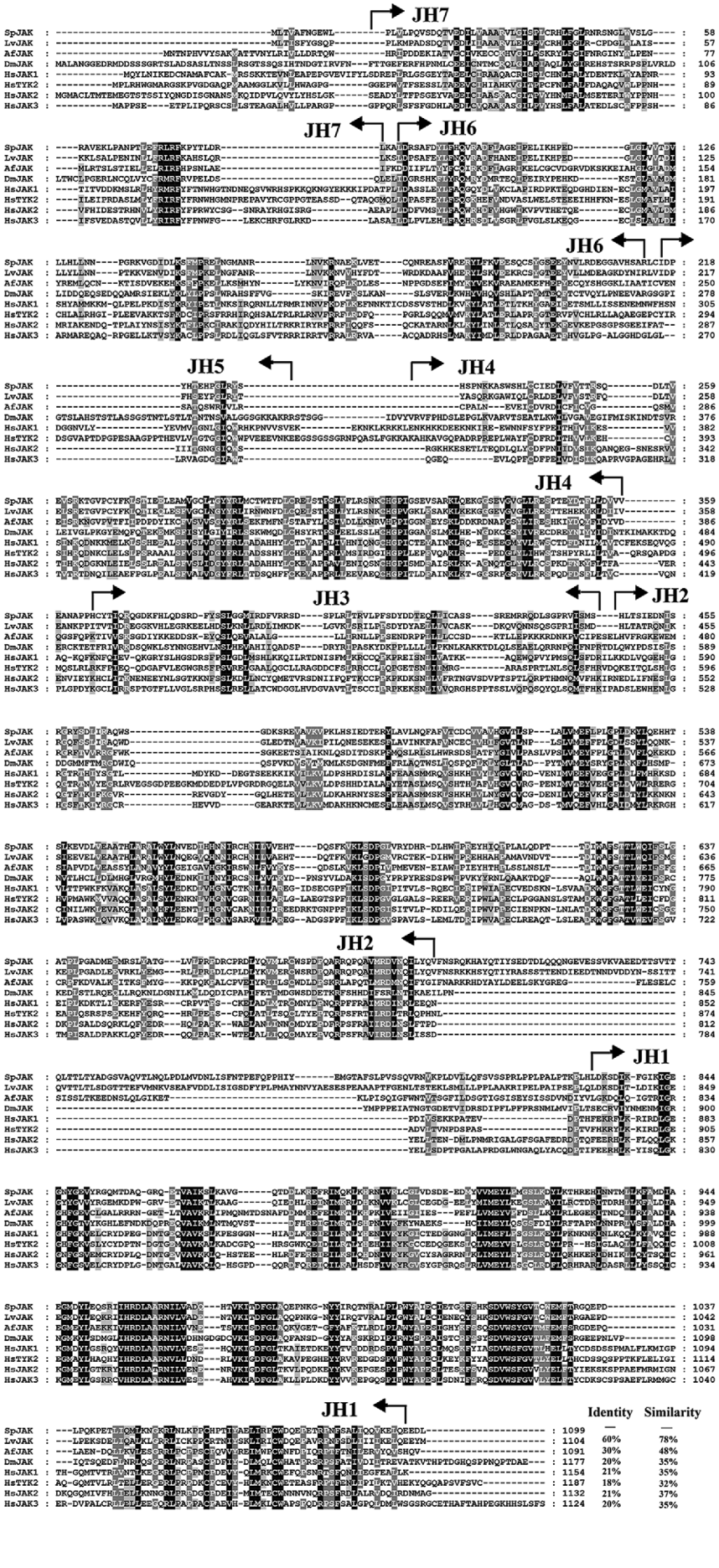

(caption on next page)

Fig. 2. Multiple sequence alignment of the JAKs from human, *drosophila* and crustaceans. The identical amino acid residues shaded in black and the similar residues in gray. Proteins analyzed listed below: LvJAK, *Litopenaeus vannamei* JAK (AKM12664.1); DmJAK, *Drosophila melanogaster* hopscotch (NP_511119.2); AfJAK, *Artemia franciscana* JAK (ACJ63722.1); HsJAK1, *Homo sapiens* JAK1 (NP_002218.2); HsJAK2, *H. sapiens* JAK2 (NP_004963.1); HsJAK3, *H. sapiens* JAK3 (NP_000206.2).

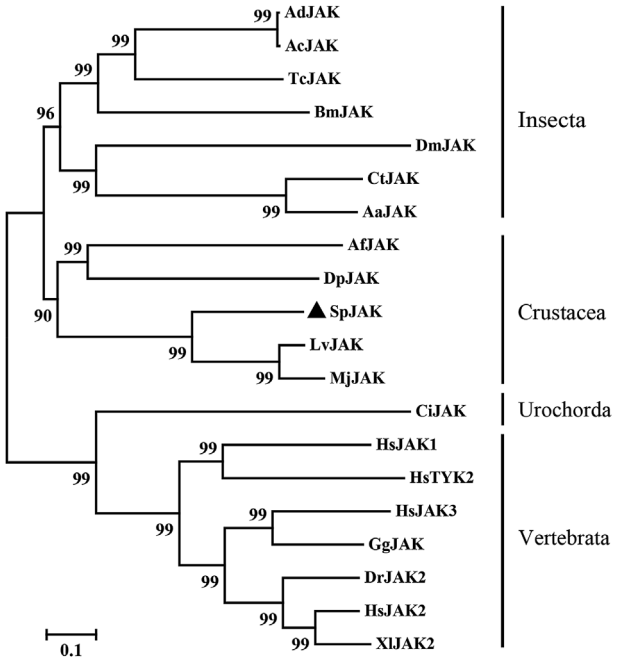

Fig. 3. Phylogenetic tree analysis of the full-length amino acid sequences of JAK proteins from various species using MEGA 5.0 software. SpJAK was marked with a triangle. Proteins analyzed listed below: SpJAK, *Scylla paramamosain* JAK (MH598509); AdJAK, *Apis dorsata* JAK (XP_006618599.1); AcJAK, *Apis cerana* JAK (PBC26622.1); TcJAK, *Tribolium castaneum* JAK (XP_008196394.1); BmJAK, *Bombyx mori* JAK (XP_004922391.1); DmJAK, *Drosophila melanogaster* hopscotch (NP_511119.2); CtJAK, *Culex tritaeniorhynchus* JAK (AAQ18517.1); AaJAK, *Aedes aegypti* JAK (EAT35265.2); AfJAK, *Artemia franciscana* JAK (ACJ63722.1); DpJAK, *Daphnia pulex* hopscotch-like protein (EFX87846.1); LvJAK, *Litopenaeus vannamei* JAK (AKM12664.1); MjJAK, *Marsupenaeus japonicus* JAK (ANA91281.1); CiJAK, *Ciona intestinalis* JAK (NP_001071749.1); HsJAK1, *Homo sapiens* JAK1 (NP_002218.2); HsJAK2, *H. sapiens* JAK2 (NP_004963.1); Hs JAK3, *H. sapiens* JAK3 (NP_000206.2); HsTYK2, *H. sapiens* TYK2 (NP_003322); GgJAK, *Gallus gallus* JAK (AAC34195.1); DrJAK2, *Danio rerio* JAK2 (NP_571162.1); XlJAK2, *Xenopus laevis* JAK2 (NP_001085288.3).

3.3. Subcellular localization analysis

To determine the subcellular localization of *Sp*JAK and its mutants, we constructed and transfected the V5-tagged plasmids into S2 cells. We analyzed subcellular localization through confocal laser scanning microscopy. *Sp*JAK was dispersed in the cytoplasm, suggesting that it was cytoplasmically localized (Fig. 4A). *Sp*JAKmut1, *Sp*JAKmut2, and *Sp*JAKmut3 were also dispersed in the cytoplasm (Fig. 4A), suggesting that the mutations did not affect the subcellular localization of *Sp*JAK.

To determine whether *Sp*JAK could activate *Sp*STAT and translocate from the cytoplasm to the nucleus, we cotransfected S2 cells with equal quantities of *Sp*STAT-GFP and V5-tagged plasmid of *Sp*JAK or its mutant and pAc5.1/V5-His A (as control). We analyzed the expression of *Sp*JAK through western blotting. The results showed that V5-tagged plasmid of *Sp*JAK and its mutants were all expressed in the co-transfected cells (Fig. S1). We also analyzed the subcellular localization of *Sp*JAK, its mutants and *Sp*STAT through confocal laser scanning microscopy. After cotransfection, *Sp*JAK or its mutant was expressed in the cells that expressed the *Sp*STAT-GFP protein, and *Sp*STAT was largely translocated from the cytoplasm to the nucleus (Fig. 4B). *Sp*STAT was mostly dispersed in the cytoplasm and present in a very small amount in the nucleus in the control (Fig. 4B). This finding indicates that *Sp*JAK could activate *Sp*STAT and translocate from the cytoplasm to the nucleus in S2 cells. The levels of *Sp*STAT expression and nuclear translocation in the *Sp*JAKmut3-transfected cells is significantly lower than those in *Sp*JAK, *Sp*JAKmut1, and *Sp*JAKmut2-transfected cells (Fig. 4B). Thus, the mutation of *Sp*JAKmut3 affects the activation of *Sp*JAK to *Sp*STAT.

3.4. SpJAK activates the JAK/STAT pathway in mud crab

The promoter of the wsv069 (ie1) gene of WSSV contains a STAT-binding motif and can be activated by the JAK/STAT pathway in shrimp [42]. To investigate whether *Sp*STAT could enhance the activity of the promoter of the WSSV wsv069 gene, we conducted dual-luciferase reporter assays. Overexpression of *Sp*STAT increased the activities of the wsv069 promoter by 4.79-fold (Fig. 5), suggesting that *Sp*STAT could significantly enhance the activity of the promoter of the WSSV wsv069 gene ($p < 0.01$).

To investigate the effect of *Sp*JAK on the JAK/STAT pathway, we investigated the effect of *Sp*JAK and its mutants on the wsv069 promoter through dual-luciferase reporter assays. Compared with the pAc5.1/V5-His A transfected control group, overexpression of *Sp*JAK, *Sp*JAKmut1, *Sp*JAKmut2, and *Sp*JAKmut3 increased the activities of the wsv069 promoter by 12.5-, 13.3-, 15.6-, and 10.0-fold, respectively (Fig. 5). The activation effect of *Sp*JAK on the wsv069 promoter is similar to that of *Sp*JAKmut1 and is higher than that of *Sp*JAKmut3 (both $p < 0.01$, Fig. 5). The effect of *Sp*JAKmut2 on the wsv069 promoter is significantly higher than that of the other mutants (all $p < 0.01$, Fig. 5).

Meanwhile, to investigate whether *Sp*JAK could bind to the promoter of the wsv069 gene, the EMSA experiment was performed to detect the interaction of *Sp*JAK and the promoter of the wsv069 gene. The results showed that shift bands of protein-DNA complex were not detected when cell lysates containing recombinant *Sp*JAK were incubated with biotin-labeled DNA probes(Fig. S2). The EMSA results demonstrated that recombinant *Sp*JAK could not bind to the wsv069 promoters.

3.5. Expression of SpJAK in healthy and immune-challenged mud crab

In healthy mud crab, *Sp*JAK showed high expression in the brain, nerve, and intestine; moderate expression in most tested tissues, including gill, stomach, eyestalk, hepatopancreas, heart, and hemocyte; and low expression in muscle (Fig. 6A). After the MCRV challenge, the expression of *Sp*JAK was upregulated in the mud crab gills at 4 h, decreased to the baseline at 8 h, increased and reached the peak of 2.1-fold at 36 h, abruptly decreased at 48 h, and recovered to high levels at 72–96 h (Fig. 6B). After poly (I:C) challenge, *Sp*JAK expression was slightly downregulated at 4 h, abruptly increased and reached the peak of 1.72-fold at 24 h, then decreased and maintained a constant expression profile at 36–96 h (Fig. 6C). In response to the LPS challenge, the *Sp*JAK expression was downregulated by 49% compared with that at 0 h, persistently increased and reinstated to exceed the baseline at 4–12 h, dramatically decreased at 24 h, persistently upregulated and reached the peak level at 72 h (1.65-fold), and returned to the baseline level at 96 h (Fig. 6D). During the *S. aureus* challenge, *Sp*JAK expression was slowly increased, reached the peak of 1.86-fold at 48 hpi, and persistently decreased at 72–96 h (Fig. 6E). The *Sp*JAK expression was slightly downregulated at 4 h, abruptly increased at 8 h, maintained a high level at 12–72 h, and decreased at 96 h post *V. parahaemolyticus* challenge (Fig. 6F).

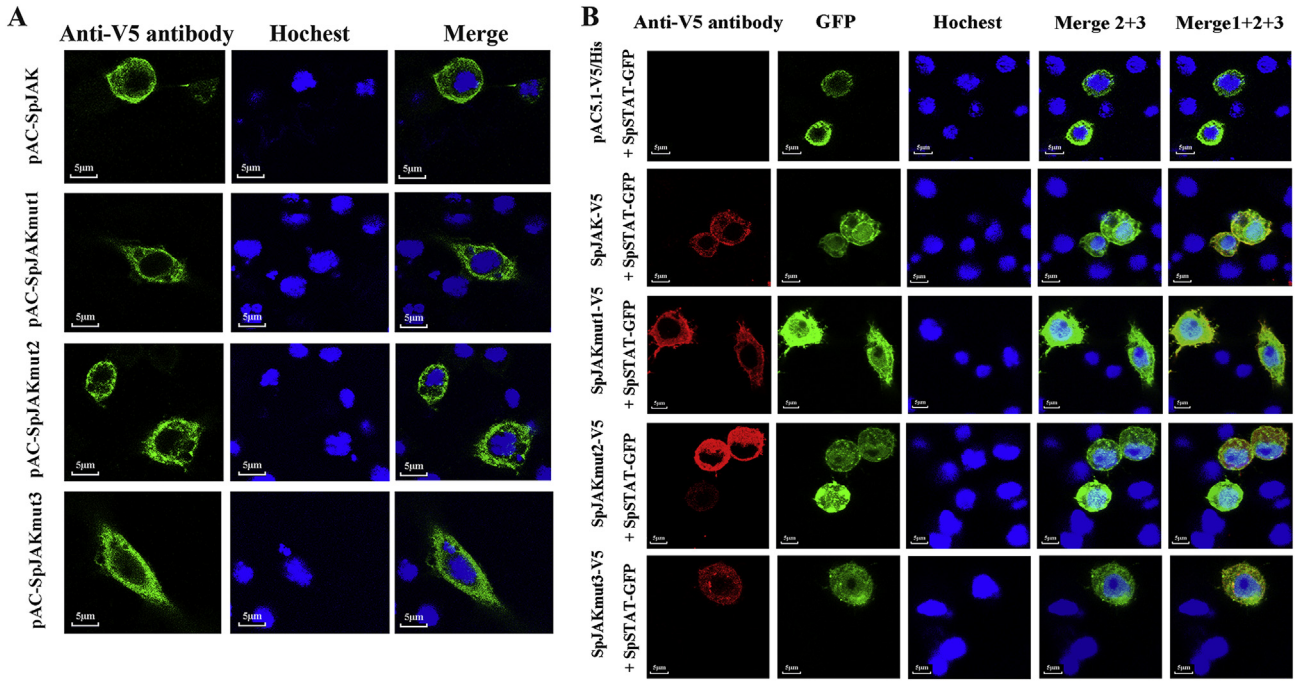

Fig. 4. Subcellular localization of *Sp*JAK and *Sp*STAT. (A) S2 cells were transfected V5-tagged *Sp*JAK and its mutants. At 48 h cells were subjected to indirect fluorescent assay (IFA) using *anti*-V5 antibody (green). The cell nucleus was stained with Hoechst33342 (blue). The merged image represents the digital superimposition of green and blue signals. (B) S2 cells were co-transfected GFP-tagged *Sp*STAT and V5-tagged *Sp*JAK, its mutants and control pAc-V5. At 48 h, the localization of GFP-tagged *Sp*STAT were observed using a Leica laser scanning confocal microscope. The nucleus were stained with Hoechst33342 (blue). The merged image represent the digital superimposition of green and blue signals. (For interpretation of the references to colour in this figure legend, the reader is referred to the Web version of this article.)

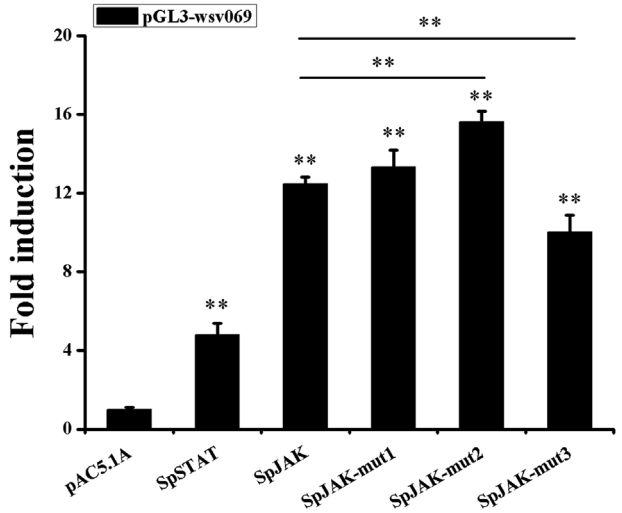

Fig. 5. Effects of *Sp*STAT, *Sp*JAK and its mutants on the promoter of WSSV wsv069 gene. Dual-luciferase reporter assays were performed on S2 cells. The detection value of the control pAc5.1/V5-His A transfected cells was used as control and set as 1.0. The bars indicate mean values ± S.D. of the luciferase activity (n = 6). **, p < 0.01.

3.6. SpJAK was involved in antiviral defense against MCRV

RNA interference assay was carried out to investigate *Sp*JAK function in *S. paramamosain*. The silencing efficiency of *Sp*JAK was evaluated on the mRNA transcript level through qPCR analysis. The mRNA level of *Sp*JAK was extremely downregulated at 48 h with 40.8% decrease after *Sp*JAK dsRNA injection; meanwhile, no suppressive effect was detected on the expression of *Sp*JAK in the gills in the GFP dsRNA and PBS injection groups (Fig. 7A). The mRNA level of *Sp*STAT was significantly downregulated at 48 h with 65.9% decrease after injection of the *Sp*JAK dsRNA and 31.5% decrease after injection of the GFP dsRNA (Fig. 7A).

Experimental mud crabs were challenged with MCRV 2 days post dsRNA-*Sp*JAK injection. During MCRV infection, the cumulative mortality rate in the dsRNA-*Sp*JAK group is significantly higher than that in the dsRNA-GFP group at 32 h post- MCRV challenge. This situation lasted until 96 h, and the gaps decreased at 128 h (logrank c2: 7.079, P < 0.01; Fig. 7B). The final mortality rates are 92.8%, 76.7%, and 90.0% for the dsRNA-*Sp*JAK, dsRNA-GFP, and PBS groups, respectively. To further evaluate the effect of *Sp*JAK knockdown on MCRV replication in mud crabs, we detected the viral copies of MCRV in the gills through absolute quantitative real-time PCR (Fig. 7C). The viral loads in the dsRNA-*Sp*JAK MCRV group are significantly higher than those in the dsRNA-GFP control group by 77.14-, 32.94-, and 21.09-fold at 48, 72, and 96 h, respectively (Fig. 7C). The MCRV genome copies and cumulative mortality in the PBS control group are significantly higher than those in the dsRNA-GFP group (Fig. 7B and C). The MCRV genome copies in the PBS control group are significantly lower than those in the dsRNA-*Sp*JAK group at 48 h (P < 0.01) and 96 h (P < 0.05) but show no significantly different at 72 h (P > 0.05). The mortality rate in the PBS control group is not significantly different with that in the dsRNA-*Sp*JAK group (P > 0.05). Hence, *Sp*JAK could play an important role in antiviral defense against MCRV.

4. Discussion

In this study, a homolog of a Janus kinase gene from *S. paramamosain* was cloned and characterized. The gene contains a conserved protein domain. *Sp*JAK could significantly activate *Sp*STAT to translocate to the nucleus and significantly enhance the activity of the promoter of the WSSV wsv069 gene, which could be significantly activated by *Sp*STAT. Hence, *Sp*JAK could activate the JAK/STAT pathway. Furthermore, the *Sp*JAK expression in the gills was significantly

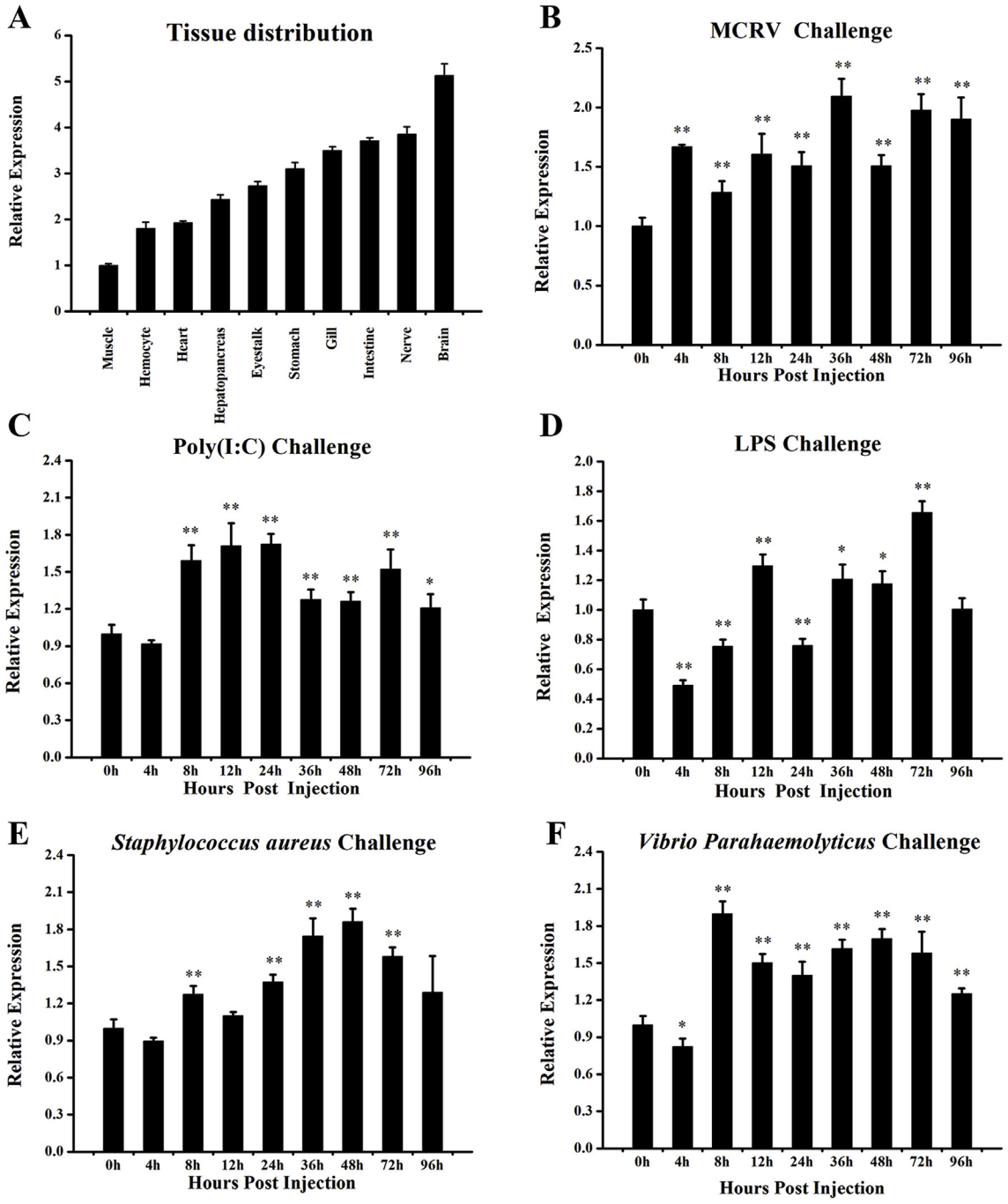

Fig. 6. Tissue distribution of *Sp*JAK in healthy mud crabs and expression profiles of *Sp*JAK after immune challenges. Real-time PCR was performed to detect expression of *Sp*JAK using the Livak (2-△△CT) method. Data were normalized to those of 18SrRNA and provided as the means ± SD of triplicate assays.(A) Tissue distribution of *Sp*JAK in healthy *S.paramamosain*. The lowest expression level in the muscle was used as control and set to 1.0. (B–F) Expression profiles of *Sp*JAK in gills from MCRV (B), Poly (I:C) (C), LPS (D), *S. aureus* (E) and *V. parahaemolyticus* (F) challenged mud crabs. Expression level detected at 0 h post injection of each group was set as 1.0. *, $p < 0.05$, **, $p < 0.01$.

upregulated by stimulation with MCRV, poly(I:C), and *V. parahaemolyticus*. Silencing *Sp*JAK *in vivo* resulted in high mortality rate and viral load in the tissues of MCRV-infected mud crabs. Thus, *Sp*JAK could play antiviral roles against MCRV infection by activating the JAK/STAT signaling pathways.

The JAK/STAT pathway is evolutionarily conserved in antiviral immunity in animals from human to *Drosophila* [9]. JAK proteins usually consist of an FERM domain, an SH2 domain, a pseudokinase domain, and a TyrKc domain. Domain prediction analysis revealed that *Sp*JAK contains an FERM domain, an SH2 domain, and two TyrKc domains from the N-terminus to C-terminus (Fig. 1B). The structure of *Sp*JAK is similar to those of *Lv*JAK [29] and *A. franciscana* JAK [34], which lacks the GXGXXG motif in the first TyrKc domain (pseudokinase domain) in contrast to *H. sapiens* JAK2 and *D. melanogaster* JAK [38]. Multiple sequence alignment revealed that *Sp*JAK displayed high similarity with *L. vannamei* JAK and *D. melanogaster* JAK, suggesting that JAK proteins were conserved in evolution and thus might have similar functions among animals.

JAKs are associated with the intracellular portion of transmembrane receptors in the cytoplasm [9]. Upon ligand binding and cytokine

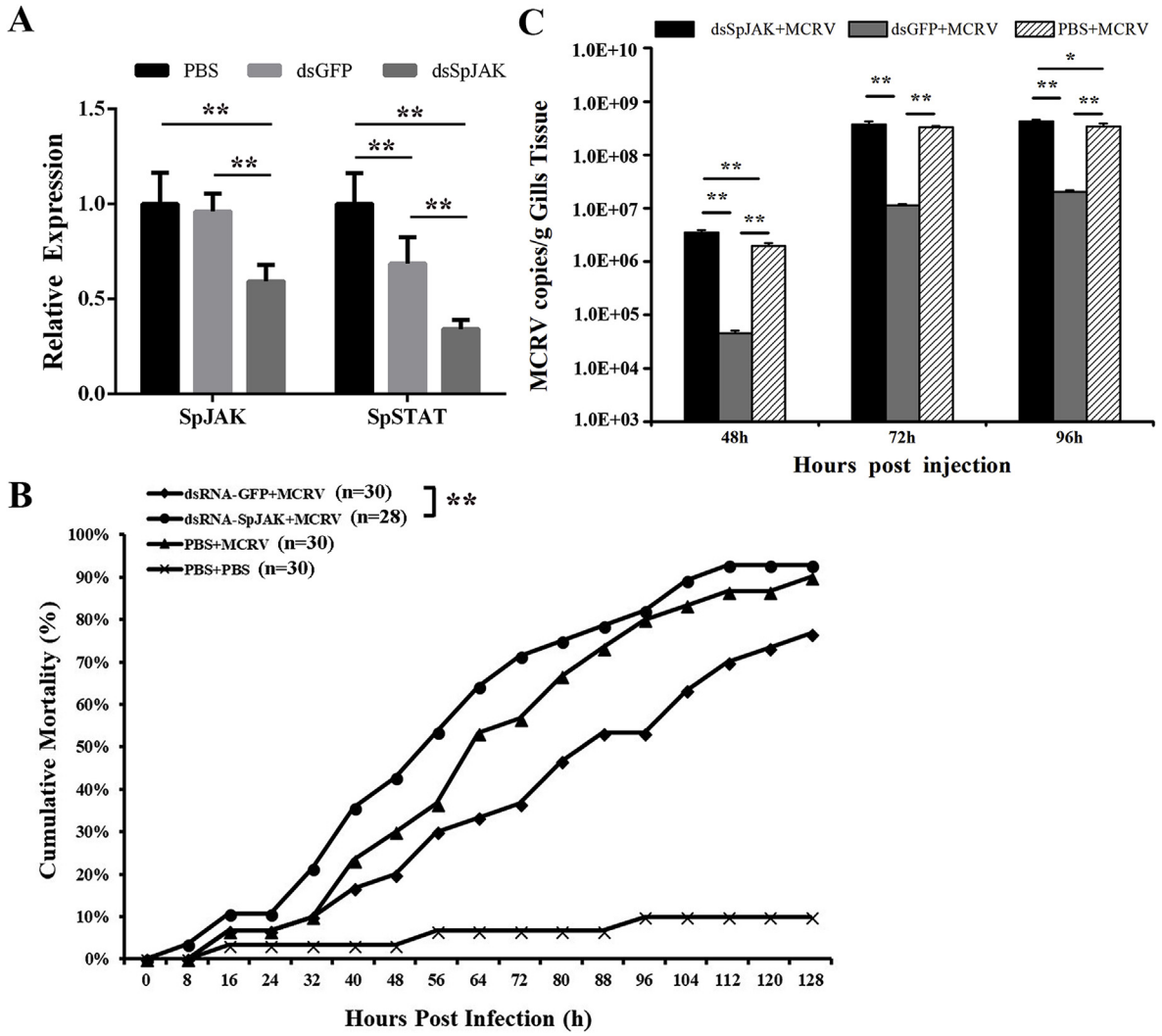

Fig. 7. Functional analysis of *Sp*JAK in MCRV infection. (A) Real-time PCR analysis of gene expression of *Sp*JAK and *Sp*STAT at 48 h after injection with indicated dsRNA or PBS. The internal control was 18SrRNA. (**,$p < 0.01$); (B) Mortalities of *Sp*JAK-silencing mud crabs were infected with MCRV. At 48 h after injection with indicated dsRNA or PBS, mud crabs were infected with MCRV and mock infected with PBS. Mortalities were recorded every 8 h. Differences in cumulative mortalities between treatments were analyzed by *Kaplane*-Meier plot (log-rank X^2 test) (*,$p < 0.05$); (C) MCRV genome copies in gill tissues (1 g) of *Sp*JAK dsRNA and control PBS and GFP dsRNA treated mud crabs at 48, 72 and 96 h post infection. Bars indicate the mean ± SD and statistical significances were calculated by the Student's t-test (**,$p < 0.01$).

receptor dimerization, the associated JAK molecules become active and transmit signaling to STATs to activate nuclear translocation [9]. Thus, cytoplasmical localization of JAK is essential for the JAK protein to exert its biological functions. In this study, the *Sp*JAK protein was dispersed in the cytoplasm as predicted and is similar to *Lv*JAK [29] and *A. franciscana* JAK [34]. This observation is consistent with the putative function of JAK as the signal transducer between the receptor and transcription factor in JAK/STAT signaling. Similarly, *Drosophila* HOP could activate the JAK/STAT pathway by activating *Dm*STAT to translocate to the nucleus [38], and *Sp*JAK could significantly activate *Sp*STAT to translocate to the nucleus. Hence, *Sp*JAK could activate the JAK/STAT pathway. The promoter of the wsv069 (ie1) gene of WSSV contains a STAT-binding motif and can be activated by the JAK/STAT pathway in shrimp [42]. In the present study, overexpression of *Sp*STAT significantly enhanced the activity of the promoter of the WSSV wsv069 gene. As such, the promoter could be activated by the JAK/STAT pathway in mud crab. Moreover, the promoter could be significantly activated by *Sp*JAK. This finding provides evidence that *Sp*JAK could activate the JAK/STAT pathway. The mammalian JAK-STAT pathway is autoregulated by inducing positive and negative regulators, and the activated STAT proteins promote their own expression [10,12,13]. Similar to mammalian STATs, STAT92E is transcriptionally induced by JAK-STAT signaling in *Drosophila* and the activated STAT92E promotes its own expression [16]. Overexpression *Sp*STAT, not being activated, was not promoted itself to largely translocated to the nucleus of *Drosophila* Schneider 2 cells (Fig. 4B). *Sp*STAT was significantly activated by *Sp*JAK and translocated to the nucleus of *Drosophila* Schneider 2 cells (Fig. 4B). STAT92E is likely to be activated by conservative *Sp*JAK in S2 cells and promotes its own expression and then enhanced the activity of the promoter of the WSSV wsv069 gene. These reasons are the possible explanations why the *Sp*JAK, not being able to be bound with the wsv069 promoter (Fig. S2), can activate the promoter activity of the wsv069 gene, which significantly higher than that the *Sp*STAT protein can activate. This result further provides evidence that *Sp*JAK could activate the JAK/STAT pathway.

Analysis of *Sp*JAK specific transcriptional regulation and cellular responses was performed following immunostimulant exposure to further understand the defense mechanisms of mud crab. The expression of genes related to the JAK/STAT signal pathway changed after administering various immunostimulants. The expression of *Lv*JAK was prominently upregulated after the stimulation of poly (I:C) and WSSV challenge [29]. The expression of the JAK family members of mandarin

fish were increased to certain extent by poly(I:C) in MFF-1 cells [43]. The SOCS in the Chinese mitten crab was also upregulated after stimulation with Gram-positive bacteria [44]. In the present study, *Sp*JAK was upregulated in response to exposure to pathogens and immunostimulants, including MCRV, *V. parahaemolyticus*, *S. aureus*, Poly (I: C), and LPS (Fig. 5). After the MCRV challenge, the *Sp*JAK expression was upregulated during the entire infection period, especially after 36 h. In response to the poly (I:C) challenge, the *Sp*JAK expression was upregulated at 8–24 h. During LPS treatment and *S. aureus* challenge, the *Sp*JAK expression was downregulated in the early stage but was significantly upregulated at 36–72 h and is similar to *V. parahaemolyticus* challenge. Moreover, *Sp*JAK expression was significantly upregulated at 96 h after *V. parahaemolyticus* challenge. Hence, *Sp*JAK plays a major role in responses to stimuli, especially in the late period.

In mammals, the JAK/STAT signaling pathway was first identified due to the IFNs-mediated biological responses and found to play critical roles in regulating ISGs [45]. In *Drosophila*, Hopscotch participated in the control of the DCV load in infected flies and was required but not sufficient for inducing virus-regulated genes, such as TotM and vir-1. In shrimps, knockdown of *Lv*JAK, *Lv*STAT, and effectors TEP1 and TEP2 caused an impaired antiviral defense and resulted in high cumulative mortality rates and WSSV copies in tissues [29,46]. Overall, these results imply that the JAK/STAT pathway plays positive roles in antiviral immunity in shrimp. It has been reported that in shrimp nonspecific dsRNA can trigger an antiviral response [47]. In this study, the MCRV genome copies and cumulative mortality in the PBS control group are higher than those in the dsRNA-GFP group. This prompted us to address the possibility that, as in shrimps, dsRNA can induce an antiviral immunity in mud crabs. In the present study, dsRNA-mediated gene silencing was used to determine the roles of *Sp*JAK during MCRV infection. The cumulative mortality rates of *Sp*JAK-knockdown mud crabs are higher than those of the GFP dsRNA (the control group) injected mud crabs after MCRV infection. Hence, *Sp*JAK could play an important role in antiviral defense against MCRV. Furthermore, the MCRV copies of *Sp*JAK-silenced mud crabs are higher than those in the control (GFP dsRNA injected group), consistent with the mortality rate experiment. Previous study indicated that all nucleic acids tested, including dsRNA mimics poly(C:G) and poly(I:C), ssRNA mimics CL097 and poly C, and DNA mimic CpG-DNA ODN2006, could provide antiviral protection for these shrimp after they were challenged with WSSV [48]. This report was in good agreement with our results that the cumulative mortality and MCRV copies were higher in the PBS injected mud crabs than those in the GFP dsRNA injected mud crabs. Similar to shrimps [29], the cumulative mortality and WSSV copies were higher in the PBS injected shrimps than those in the GFP dsRNA injected group. These results suggest that *Sp*JAK could play an important role in antiviral defense against MCRV. This work is the first to report that the complete set of JAK/STAT proteins could activate the JAK/STAT pathway to restrain MCRV in *S. paramamosain*.

The FERM domain can interact with the kinase domain and positively regulate catalytic activity. Mutations within the FERM domain of JAK3 dampen or augment kinase activity [46,49,50]. The Src homology 2 (SH2)-like domains (JH3 and JH4) play a structural role in interaction with receptor and the TyrKc domain, but a mutation on the SH2 domain of JAK1 does not interfere with its kinase activity or receptor association [51,52]. Despite the lack of catalytic activity, the pseudo-kinase domain is required for suppression of basal activity of tyrosine kinases and cytokine-inducible activation of signal transduction. Some mutations in this domain could positively or negatively regulate JAK kinase activity, resulting in human diseases [53–55]. A number of mutations in the JAK3 domain could enhance the enzymatic activity of JAK3 [56,57]. RTKs are usually activated through ligand binding, which causes dimerization and autophosphorylation of the intracellular Tyr kinase catalytic domain, leading to intracellular signaling. The kinase activity of these proteins depends on their phosphorylation at the tyrosine residues in the activation loop of the kinase domain. Aberrant expression of PTKs is associated with many developmental abnormalities and cancers. In the present study, deletion mutation on the FERM domain of *Sp*JAK slightly augmented the kinase activity ($P > 0.05$). Deletion mutations on the SH2 domain significantly enhanced the kinase activity ($P < 0.01$). Deletion mutation on the SH2 domain inhibited the function of the pseudo-kinase domain, thereby suppressing the basal activity of tyrosine kinases and enhancing the tyrosine kinase activity. This finding is worthy of further studies. The first tyrosine kinases, catalytic domain mutation, considerably inhibited the activity of JAK kinase because this domain contains phosphorylation sites that are essential for the kinase activity of JAK proteins.

RNA interference (RNAi), a huge breakthrough in modern molecular biology, uses exogenous double-strand RNA (dsRNA) to trigger sequence-specific gene silencing [58,59]. At present, RNAi has become a widely used tool for analysis of gene functions in organisms, including crabs. The efficiency of RNAi in arthropods can be influenced by several factors including dsRNA concentration, sequence and length of dsRNA, persistence of gene silencing, insect life-stage, and target gene and dsRNA fragment [60–65]. In addition, 73.8% of the total reads of the siRNA duplexes (22 nt) of the HEV71D23A-derived siRNAs were concentrated at the 5′ termini of the HEV71 genome. Notably, 94.9% of the negative-stranded vsRNA reads 22 nt in size were derived from the terminal regions of antigenomic RNAs [66]. In the present study, the mRNA level of *Sp*JAK was downregulated by 40.8% at 48 h after *Sp*JAK dsRNA injection; meanwhile, the efficiency of RNAi is lower than that of silencing *Sp*TRAF6 [31] and *Lv*DOME at 72 h post dsRNA injection [42]. The selected dsRNA fragment is far from the 5′ termini of the *Sp*JAK genome or the time for detecting the efficiency of RNAi is earlier than that of *Sp*TRAF6 and *Lv*DOME. Moreover, the experimental mud crabs used in this study may be bigger than those used in the silencing of *Sp*TRAF6. This finding is worthy of further studies. The mRNA level of *Sp*STAT was downregulated by 31.5% after injection of the GFP dsRNA possibly because of the siRNA-mediated silencing of numerous unintended (off-target) transcripts. Sequence analysis showed that several regions of more than 11 nt consecutive sequence of *Sp*STAT are complementary with the sequence of dsRNA-GFP. Sequence analysis of several off-target transcripts revealed only partial (11–13 nt) complementarity with the transfected siRNAs [67]. The generation of off-target gene silencing via the 7 nt motif depends on the characteristics of the target mRNA, including the sequence context surrounding the complementary region, the position of the complementary region in the mRNA, and the copy number of the complementary region. No algorithm can eliminate significant numbers of 7–8 base matches of siRNAs to the transcriptome, and perfect specificity will be difficult to achieve [68]. The mammalian JAK-STAT pathway is autoregulated by inducing positive and negative regulators, and the activated STAT proteins promote their own expression [10,12,13]. Similar to mammalian STATs, STAT92E is transcriptionally induced by JAK-STAT signaling in *Drosophila* and promotes its own expression [16]. In the present study, the expression of *Sp*STAT was significantly downregulated by 65.9% after injection of *Sp*JAK dsRNA. The reason that JAK knockdown leads to decreased the expression of *Sp*STAT is that there may be JAK affecting the signal pathway STAT expresses, ror *Sp*STAT activated by *Sp*JAK affects their own expression in mud crab, which is worthy of further studies.

Acknowledgment

This research was supported by the National Natural Science Foundation of China under grant Nos. 31672677 and China Agriculture Research System(CARS-48). The funders had no role in study design, data collection and analysis, decision to publish, or preparation of the manuscript.

Appendix A. Supplementary data

Supplementary data related to this article can be found at https://doi.org/10.1016/j.fsi.2019.03.056.

References

[1] S. Weng, Z. Guo, J. Sun, S. Chan, J. He, A reovirus disease in cultured mud crab, *Scylla serrata*, in southern China, J. Fish Dis. 30 (2007) 133–139.
[2] Fisheries Bureau of the Ministry of Agriculture of China, China Fishery Yearbook 2017, China agriculture press, Beijing, 2017, p. 22.
[3] X.X. Deng, L. Lu, Y.J. Ou, H.J. Su, G. Li, Z.X. Guo, et al., Sequence analysis of 12 genome segments of mud crab reovirus (MCRV), Virology 422 (2012) 185–194.
[4] T.J. Little, D. Hultmark, A.F. Read, Invertebrate immunity and the limits of mechanistic immunology, Nat. Immunol. 6 (2005) 651–654.
[5] H. Kiu, S.E. Nicholson, Biology and significance of the JAK/STAT signaling pathways, Growth Factors 30 (2012) 88–106.
[6] J.S. Rawlings, K.M. Rosler, D.A. Harrison, The JAK/STAT signaling pathway, J. Cell Sci. 117 (2004) 1281–1283.
[7] G.R. Stark, J.E. Darnell Jr., The JAK-STAT pathway at twenty, Immunity 36 (2012) 503–514.
[8] G.C. Sen, Viruses and interferons, Annu. Rev. Microbiol. 55 (2001) 255–281.
[9] W.X. Li, Canonical and non-canonical JAK-STAT signaling, Trends Cell Biol. 18 (2008) 545–551.
[10] K. Shuai, B. Liu, Regulation of JAK-STAT signaling in the immune system, Nat. Rev. Immunol. 3 (2003) 900–911.
[11] D.S. Aaronson, C.M. Horvath, A road map for those who don't know JAK-STAT, Science 296 (2002) 1653–1655.
[12] D.E. Levy, J.E. Darnell Jr., Stats: transcriptional control and biological impact, Nat. Rev. Mol. Cell Biol. 3 (2002) 651–662.
[13] N.I. Arbouzova, M.P. Zeidler, JAK/STAT signaling in Drosophila: insights into conserved regulatory and cellular functions, Development 133 (2006) 2605–2616.
[14] X.S. Hou, et al., Marelle acts downstream of the *Drosophila* HOP/JAK kinase and encodes a protein similar to the mammalian STATs, Cell 84 (1996) 411–419.
[15] R. Yan, et al., Identification of a Stat gene that functions in *Drosophila* development, Cell 84 (1996) 421–430.
[16] R. Xi, et al., A gradient of JAK pathway activity patterns the anterior-posterior axis of the follicular epithelium, Dev. Cell 4 (2003) 167–177.
[17] B.A. Callus, B. Mathey-Prevot, SOCS36E, a novel *Drosophila* SOCS protein, suppresses JAK/STAT and EGF-R signaling in the imaginal wing disc, Oncogene 21 (2002) 4812–4821.
[18] P. Karsten, et al., Cloning and expression of *Drosophila* SOCS36E and its potential regulation by the JAK/STAT pathway, Mech. Dev. 117 (2002) 343–346.
[19] J.S. Rawlings, et al., Two *Drosophila* suppressors of cytokine signaling (SOCS) differentially regulate JAK and EGFR pathway activities, BMC Cell Biol. 5 (2004) 38.
[20] G.H. Baeg, et al., Genome-wide RNAi analysis of JAK/STAT signaling components in *Drosophila*, Genes Dev. 19 (2005) 1861–1870.
[21] M.J. De Veer, M. Holko, M. Frevel, E. Walker, S. Der, J.M. Paranjape, R.H. Silverman, B.R. Williams, Functional classification of interferon-stimulated genes identified using microarrays, J. Leukoc. Biol. 69 (2001) 912–920.
[22] A.J. Sadler, B.R.G. Williams, Interferon-inducible antiviral effectors, Nat. Rev. Immunol. 8 (2008) 559–568.
[23] C. Dostert, E. Jouanguy, P. Irving, L. Troxler, D. Galiana-Arnoux, C. Hetru, J.A. Hoffmann, J.-L. Imler, The JAK-STAT signaling pathway is required but not sufficient for the antiviral response of *drosophila*, Nat. Immunol. 6 (2005) 946–953.
[24] B. Lemaitre, J. Hoffmann, The host defense of *Drosophila melanogaster*, Annu. Rev. Immunol. 25 (2007) 697–743.
[25] J. Xu, S. Cherry, Viruses and antiviral immunity in *Drosophila*, Dev. Comp. Immunol. 42 (2014) 67–84.
[26] W.Y. Chen, K.C. Ho, J.H. Leu, K.F. Liu, H.C. Wang, G.H. Kou, C.F. Lo, WSSV infection activates STAT in shrimp, Dev. Comp. Immunol. 32 (2008) 1142–1150.
[27] S.-J. Lin, H.-L. Hsia, W.-J. Liu, J.-Y. Huang, K.-F. Liu, W.-Y. Chen, Y.-C. Yeh, Y.-T. Huang, C.-F. Lo, G.-H. Kou, H.-C. Wang, Spawning stress triggers WSSV replication in brooders via the activation of shrimp STAT, Dev. Comp. Immunol. 38 (2012) 128–135.
[28] S. Okugawa, T. Mekata, M. Inada, K. Kihara, A. Shiki, K. Kannabiran, T. Kono, M. Sakai, T. Yoshida, T. Itami, R. Sudhakaran, The SOCS and STAT from JAK/STAT signaling pathway of kuruma shrimp *Marsupenaeus japonicus*: molecular cloning, characterization and expression analysis, Mol. Cell. Probes 27 (2013) 6–14.
[29] X. Song, Z. Zhang, S. Wang, H. Li, H. Zuo, X. Xu, S. Weng, J. He, C. Li, A Janus kinase in the JAK/STAT signaling pathway from *Litopenaeus vannamei* is involved in antiviral immune response, Fish Shellfish Immunol. 44 (2015) 662–673.
[30] Sheng Wang, Xuan Song, Zijian Zhang, Jianguo He, Chaozheng Li, et al., Shrimp with knockdown of LvSOCS2, a negative feedback loop regulator of JAK/STAT pathway in *Litopenaeus vannamei*, exhibit enhanced resistance against WSSV, Dev. Comp. Immunol. 65 (2016) 289–298.
[31] Wanwei Sun, Xinxu Zhang, Weisong Wan, Shuqi Wang, Shengkang Li, et al., Tumor necrosis factor receptor-associated factor 6 (TRAF6) participates in anti-lipopolysaccharide factors (ALFs) gene expression in mud crab, Dev. Comp. Immunol. 67 (2017) 361–376.
[32] Z. Lin, J. Qiao, Y. Zhang, L. Guo, H. Huang, F. Yan, Y. Li, X. Wang, Cloning and characterisation of the SpToll gene from green mud crab, *Scylla paramamosain*, Dev. Comp. Immunol. 37 (2012) 164–175.
[33] X.C. Li, X.W. Zhang, J.F. Zhou, H.Y. Ma, Z.D. Liu, L. Zhu, X.J. Yao, L.G. Li, W.H. Fang, Identification, characterization, and functional analysis of Tube and Pelle homologs in the mud crab *Scylla paramamosain*, PLoS One 8 (2013) e76728.
[34] X.C. Li, L. Zhu, L.G. Li, Q. Ren, Y.Q. Huang, J.X. Lu, W.H. Fang, W. Kang, A novel myeloid differentiation factor 88 homolog, SpMyD88, exhibiting SpToll-binding activity in the mud crab *Scylla paramamosain*, Dev. Comp. Immunol. 39 (2013) 313–322.
[35] Zhi-Qiang Du, Qian Ren, An-Ming Huang, Xin-Cang Li, et al., A novel peroxinectin involved in antiviral and antibacterial immunity of mud crab, *Scylla paramamosain*, Mol. Biol. Rep. 40 (2013) 6873–6881.
[36] Zhi Wang, Baozhen Sun, Fei Zhu, Epigallocatechin-3-gallate inhibit replication of white spot syndrome virus in *Scylla paramamosain*, Fish Shellfish Immunol. 67 (2017) 612–619.
[37] S. Liu, G. Chen, H. Xu, W. Zou, W. Yan, Q. Wang, et al., Transcriptome analysis of mud crab (*Scylla paramamosain*) gills in response to mud crab reovirus (MCRV), Fish Shellfish Immunol. 60 (2017) 545–553.
[38] C. Li, Y. Chen, S. Weng, S. Li, H. Zuo, X. Yu, et al., Presence of Tube isoforms in *Litopenaeus vannamei* suggests various regulatory patterns of signal transduction in invertebrate NF-*kappa*B pathway, Dev. Comp. Immunol. 42 (2014) 174–185.
[39] M.A. Larkin, G. Blackshields, N.P. Brown, R. Chenna, P.A. McGettigan, H. McWilliam, et al., Clustal W and clustal X version 2.0, Bioinformatics 23 (2007) 2947–2948.
[40] K. Tamura, D. Peterson, N. Peterson, G. Stecher, M. Nei, S. Kumar, MEGA5: molecular evolutionary genetics analysis using maximum likelihood, evolutionary distance, and maximum parsimony methods, Mol. Biol. Evol. 28 (2011) 2731–2739.
[41] D.R. Cavener, Comparison of the consensus sequence flanking translational start sites in *Drosophila* and vertebrates, Nucleic Acids Res. 15 (1987) 1353–1361.
[42] Muting Yan, Chaozheng Li, Ziqi Su, Jianguo He, Xiaopeng Xu, Identification of a JAK/STAT pathway receptor domeless from Pacific white shrimp *Litopenaeus vannamei*, Fish Shellfish Immunol. 44 (2015) 26–32.
[43] C.J. Guo, Y.F. Zhang, L.S. Yang, X.B. Yang, Y.Y. Wu, D. Liu, W.J. Chen, S.P. Weng, X.Q. Yu, J.G. He, The JAK and STAT family members of the Mandarin fish *Siniperca chuatsi*: molecular cloning, tissues distribution and immunobiological activity, Fish Shellfish Immunol. 27 (2009) 349–359.
[44] Y. Zhang, J. Zhao, H. Zhang, Y. Gai, L. Wang, F. Li, et al., The involvement of suppressors of cytokine signaling 2 (SOCS2) in immune defense responses of Chinese mitten crab *Eriocheir sinensis*, Dev. Comp. Immunol. 34 (2010) 42–48.
[45] C. Schindler, C. Plumlee, Interferons pen the JAK-STAT pathway, Semin. Cell Dev. Biol. 19 (2008) 311–318.
[46] Q. Ren, Y. Huang, Y. He, W. Wang, X. Zhang, A white spot syndrome virus microRNA promotes the virus infection by targeting the host STAT, Sci. Rep. 5 (2015) 18384.
[47] J. Robalino, C.L. Browdy, S. Prior, et al., Induction of antiviral immunity by double-stranded RNA in a marine invertebrate, J. Virol. 78 (2004) 10442–10448.
[48] P.-H. Wang, L.-S. Yang, Z.-H. Gu, S.-P. Weng, X.-Q. Yu, J.-G. He, Nucleic acid-induced antiviral immunity in shrimp, Antivir. Res. 99 (2013) 270–280.
[49] Wei Wu, Xiao-Hong Sun, Janus kinase 3: the controller and the controlled, Acta Biochim. Biophys. Sin. 44 (2012) 187–196.
[50] Y.J. Zhou, M. Chen, N.A. Cusack, L.H. Kimmel, K.S. Magnuson, J.G. Boyd, W. Lin, et al., Unexpected effects of FERM domain mutations on catalytic activity of JAK3: structural implication for Janus kinases, Mol. Cell 8 (2001) 959–969.
[51] N.E. Elliott, S.M. Cleveland, V. Grann, J. Janik, T.A. Waldmann, U.P. Dave, FERM domain mutations induce gain of function in JAK3 in adult T-cell leukemia/lymphoma, Blood 118 (2011) 3911–3921.
[52] S. Radtke, S. Haan, A. Jorissen, H.M. Hermanns, S. Diefenbach, T. Smyczek, H. Schmitz-Vandeleur, et al., The JAK1 SH2 domain does not fulfill a classical SH2 function in JAK/STAT signaling but plays a structural role for receptor interaction and up-regulation of receptor surface expression, J. Biol. Chem. 280 (2005) 25760–25768.
[53] H. Luo, P. Rose, D. Barber, W.P. Hanratty, S. Lee, T.M. Roberts, C.R. Dearolf, Mutation in the JAK kinase JH2 domain hyperactivates *Drosophila* and mammalian JAK-Stat pathways, Mol. Cell Biol. 17 (1997) 1562–1571.
[54] P. Saharinen, O. Silvennoinen, The pseudokinase domain is required for suppression of basal activity of JAK2 and JAK3 tyrosine kinases and for cytokine-inducible activation of signal transduction, J. Biol. Chem. 277 (2002) 47954–47963.
[55] M. Chen, A. Cheng, F. Candotti, Y.J. Zhou, A. Hymel, A. Fasth, L.D. Notarangelo, et al., Complex effects of naturally occurring mutations in the JAK3 pseudokinase domain: evidence for interactions between the kinase and pseudokinase domains, Mol. Cell Biol. 20 (2000) 947–956.
[56] D.K. Walters, T. Mercher, T.L. Gu, T. O'Hare, J.W. Tyner, M. Loriaux, V.L. Goss, et al., Activating alleles of JAK3 in acute megakaryoblastic leukemia, Cancer Cell 10 (2006) 65–75.
[57] M.G. Cornejo, M.G. Kharas, M.B. Werneck, S. Le Bras, S.A. Moore, B. Ball, M. Beylot-Barry, et al., Constitutive JAK3 activation induces lymphoproliferative syndromes in murine bone marrow transplantation models, Blood 113 (2009) 2746–2754.
[58] A. Fire, S.Q. Xu, M.K. Montgomery, S.A. Kostas, S.E. Driver, C.C. Mello, Potent and specific genetic interference by double-stranded RNA in Caenorhabditis elegans, Nature 391 (1998) 806–811.
[59] G.J. Hannon, J.J. Rossi, Unlocking the potential of the human genome with RNA interference, Nature 431 (2004) 371–378.
[60] J.A. Baum, T. Bogaert, W. Clinton, G.R. Heck, P. Feldmann, et al., Control of coleopteran insect pests through RNA interference, Nat. Biotechnol. 25 (2007) 1322–1326.
[61] S. Whyard, A.D. Singh, S. Wong, Ingested double-stranded RNAs can act as species-specific insecticides, Insect Biochem. Mol. Biol. 39 (2009) 824–832.
[62] H. Huvenne, G. Smagghe, Mechanisms of dsRNA uptake in insects and potential of

RNAi for pest control: a review, J. Insect Physiol. 56 (2010) 227–235.
[63] P. Kumar, S.S. Pandit, I.T. Baldwin, Tobacco rattle virus vector: a rapid and transient means of silencing *Manduca sexta* genes by plant mediated RNA interference, PLoS One 7 (2012).
[64] Rong Wen, Fuhua Li, Shihao Li, Jianhai Xiang, Function of shrimp STAT during WSSV infection, Fish Shellfish Immunol. 38 (2014) 354–360.
[65] R. Bolognesi, P. Rameseshadri, J. Anderson, P. Bachman, W. Clinton, R. Flannagan, et al., Characterizing the mechanism of action of double-stranded RNA activity against western corn rootworm (Diabrotica virgifera virgifera LeConte), PLoS One 7 (2012) e47534.
[66] Yang Qiu, Yanpeng Xu, Yao Zhang, Hui Zhou, Xi Zhou, et al., Human virus-derived small RNAs can confer antiviral immunity in mammals, Immunity 46 (2017) 992 100.
[67] A.L. Jackson, S.R. Bartz, J. Schelter, S.V. Kobayashi, J. Burchard, M. Mao, B. Li, G. Cavet, P.S. Linsley, Expression profiling reveals off-target gene regulation by RNAi, Nat. Biotechnol. 21 (2003) 635–637.
[68] A.L. Jackson, et al., Widespread siRNA “off-target” transcript silencing mediated by seed region sequence complementarity, RNA 12 (2006) 1179–1187.